



This is a repository copy of *Effect of temperature and aluminium on calcium (alumino)silicate hydrate chemistry under equilibrium conditions.*

White Rose Research Online URL for this paper:  
<http://eprints.whiterose.ac.uk/86598/>

Version: Supplemental Material

---

**Article:**

Myers, R.J., Provis, J.L., L'Hôpital, E. et al. (1 more author) (2014) Effect of temperature and aluminium on calcium (alumino)silicate hydrate chemistry under equilibrium conditions. *Cement and Concrete Research*, 68. 83 - 93. ISSN 0008-8846

<https://doi.org/10.1016/j.cemconres.2014.10.015>

---

**Reuse**

Unless indicated otherwise, fulltext items are protected by copyright with all rights reserved. The copyright exception in section 29 of the Copyright, Designs and Patents Act 1988 allows the making of a single copy solely for the purpose of non-commercial research or private study within the limits of fair dealing. The publisher or other rights-holder may allow further reproduction and re-use of this version - refer to the White Rose Research Online record for this item. Where records identify the publisher as the copyright holder, users can verify any specific terms of use on the publisher's website.

**Takedown**

If you consider content in White Rose Research Online to be in breach of UK law, please notify us by emailing [eprints@whiterose.ac.uk](mailto:eprints@whiterose.ac.uk) including the URL of the record and the reason for the withdrawal request.



[eprints@whiterose.ac.uk](mailto:eprints@whiterose.ac.uk)  
<https://eprints.whiterose.ac.uk/>

# Supporting information for:

## Effect of temperature and aluminium on calcium (alumino)silicate hydrate chemistry under equilibrium conditions

Rupert J. Myers <sup>1,2,a</sup>, Emilie L'Hôpital <sup>2,b</sup>, John L. Provis <sup>1,c</sup>, Barbara Lothenbach <sup>2\*</sup>

<sup>1</sup> Department of Materials Science and Engineering, University of Sheffield, S1 3JD, Sheffield,  
United Kingdom

<sup>2</sup> Laboratory for Concrete and Construction Chemistry, EMPA, Dübendorf, 8600, Switzerland

\* Corresponding author. Email [Barbara.Lothenbach@empa.ch](mailto:Barbara.Lothenbach@empa.ch)

<sup>a</sup> [rjmyers@sheffield.ac.uk](mailto:rjmyers@sheffield.ac.uk). <sup>b</sup> [Emilie.Lhopital@empa.ch](mailto:Emilie.Lhopital@empa.ch). <sup>c</sup> [j.provis@sheffield.ac.uk](mailto:j.provis@sheffield.ac.uk).

## Appendix S1. Details of the deconvolution method for the $^{29}\text{Si}$ MAS NMR spectra

The  $^{29}\text{Si}$  MAS NMR spectra were deconvoluted using the structural constraints described here, for C-(A-)S-H nanostructures with nearest-neighbour Al-O-Al avoidance [1]. A ratio of  $Q_p^2/Q_b^2 = 2$  was specified for the non-cross-linked C-(A-)S-H products, which is required for consistency with 'dreierketten-type'  $(3n-1)$  chain structures [2]. Additional constraints were specified for the cross-linked C-(A-)S-H products [3], which are:

- i)  $Q^2(1\text{Al}) \geq 2Q^3(1\text{Al})$ ;
- ii)  $Q^2 + Q^2(1\text{Al}) \geq 2(Q^3 + 2Q^3(1\text{Al}))$ ;
- iii)  $Q_p^{2*} \geq 0$ ;
- iv)  $Q^2(1\text{Al})^* \geq 0$ ; and
- v)  $Q_p^{2*}/Q_b^2 = 2$

where  $Q_p^{2*} = Q_p^2 - 2(Q^3 + Q^3(1\text{Al}))$  and  $Q^2(1\text{Al})^* = Q^2(1\text{Al}) - 2Q^3(1\text{Al})$ .

## Appendix S2. Additional details of the differential mass loss peak assignments

Additional XRD data were measured to support the differential mass loss peak assignments described in the main body of the article. These data were obtained by heating C-(A-)S-H samples (synthesised under the procedure described in section 2) in a Carbolite HTF 1700 furnace at a rate of 300°C/hour to upper and lower temperatures with respect to the differential mass loss peaks analysed here (Table S1). The samples were held at the specified temperatures for 1 hour, then cooled at a rate of ~30°C/minute to room temperature under laboratory atmosphere, and subsequently stored in a desiccator (for up to 6 hours in the presence of SiO<sub>2</sub> gel) until analysis.

Table S1. Lower and upper temperatures to which C-(A-)S-H samples were heated for analysis of differential mass loss peaks (Figure 3 and shown here). Ca/Si\* = bulk Ca/Si. Al/Si\* = bulk Al/Si.

Ca/Si*	Al/Si*	Equilibration temperature (°C)	Differential mass loss peak temperature (°C)	Lower temperature (°C)	Upper temperature (°C)
1	0.1	80	~500	320	600
1	0.05	50	~380	250	520
1	0	50	~810	550-650	950
1	0.1	50	~810	550-650	950

Figure S1 shows that heating the C-A-S-H samples equilibrated at 80°C with bulk Al/Si = 0.1 to 600°C, and heating the 50°C C-A-S-H samples with bulk Al/Si = 0.05 to 520°C, results in the decomposition of C-A-S-H only. Heating these samples to 250°C (Figure S1B) or 320°C (Figure S1A) transforms C-A-S-H to a phase with similar long-range order to 9 Å tobermorite (represented by C<sub>3</sub> in Figure S1, Ca<sub>5</sub>Si<sub>6</sub>O<sub>16</sub>(OH)<sub>2</sub>, PDF# 04-012-1761) [4]. The C-A-S-H phase loses some structural similarity to 9 Å tobermorite on further heating to 520°C (Figure S1B) or

600°C (Figure S1A), which can be identified by the shift of the major 9 Å tobermorite reflections (~29.5° 2θ) to higher angles.

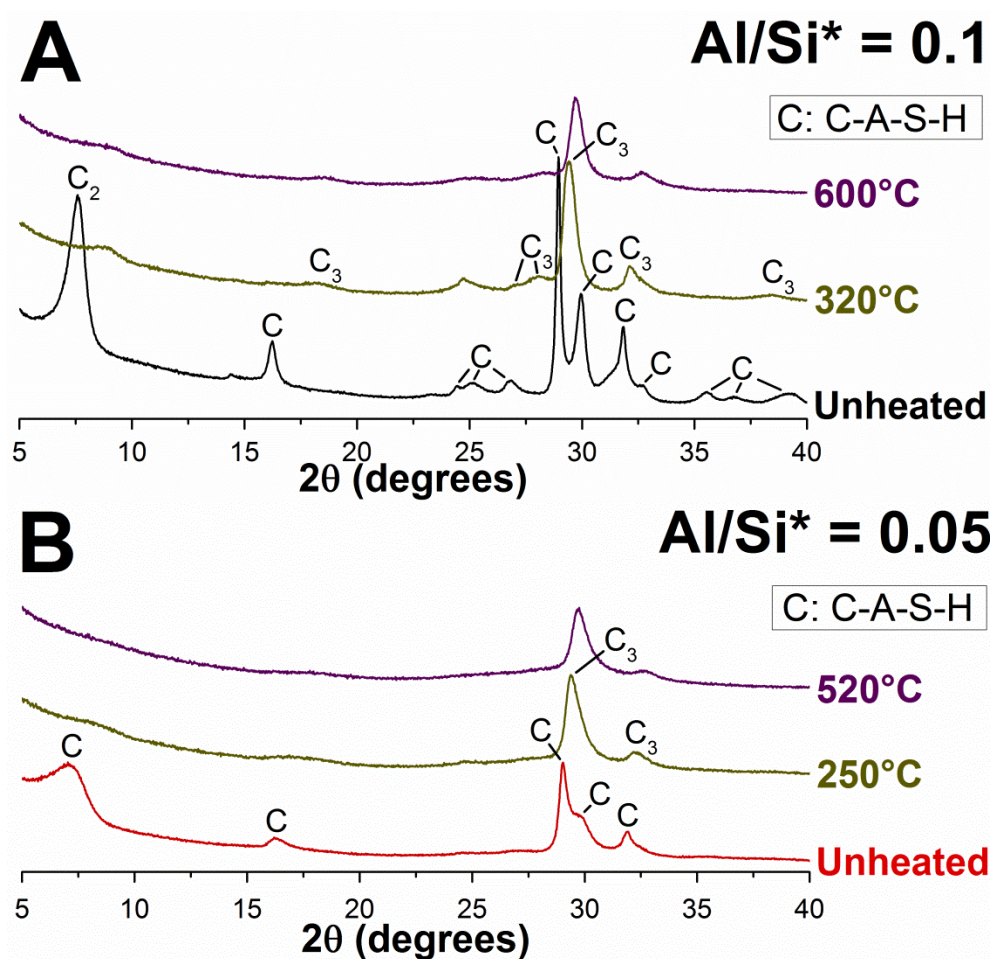


Figure S1. Cu K $\alpha$  diffractograms of C-A-S-H samples with A) bulk Al/Si = 0.1 and equilibrated at 80°C, and B) bulk Al/Si = 0.05 and equilibrated at 50°C, heated to the temperatures shown in the plots.

Figure S2 shows Cu K $\alpha$  diffractograms for C-(A-)S-H samples equilibrated at 50°C and heated to 550-650°C and 950°C (bulk Al/Si = 0 and 0.1). Decomposition of C-(A-)S-H occurs up to 550-650°C, which is shown by the loss of the  $d_{(002)}$  basal spacing peaks and shifting of the major reflections at ~29° 2θ to higher angles. Formation of a small amount of mayenite ( $C_{12}A_7$ , PDF# 00-009-0413) is observed in the bulk Al/Si = 0.1 sample during heating to/at 550-650°C (Figure

S2B). Wollastonite ( $\text{CaSiO}_3$ , PDF# 01-076-0925) is formed and decomposition of C-(A-)S-H occurs during heating between 550-650°C and 950°C; complete decomposition of C-(A-)S-H is attained after heating at 950°C for 1 hour. Mayenite is also formed in the C-A-S-H sample during heating at 950°C (Figure S2B).

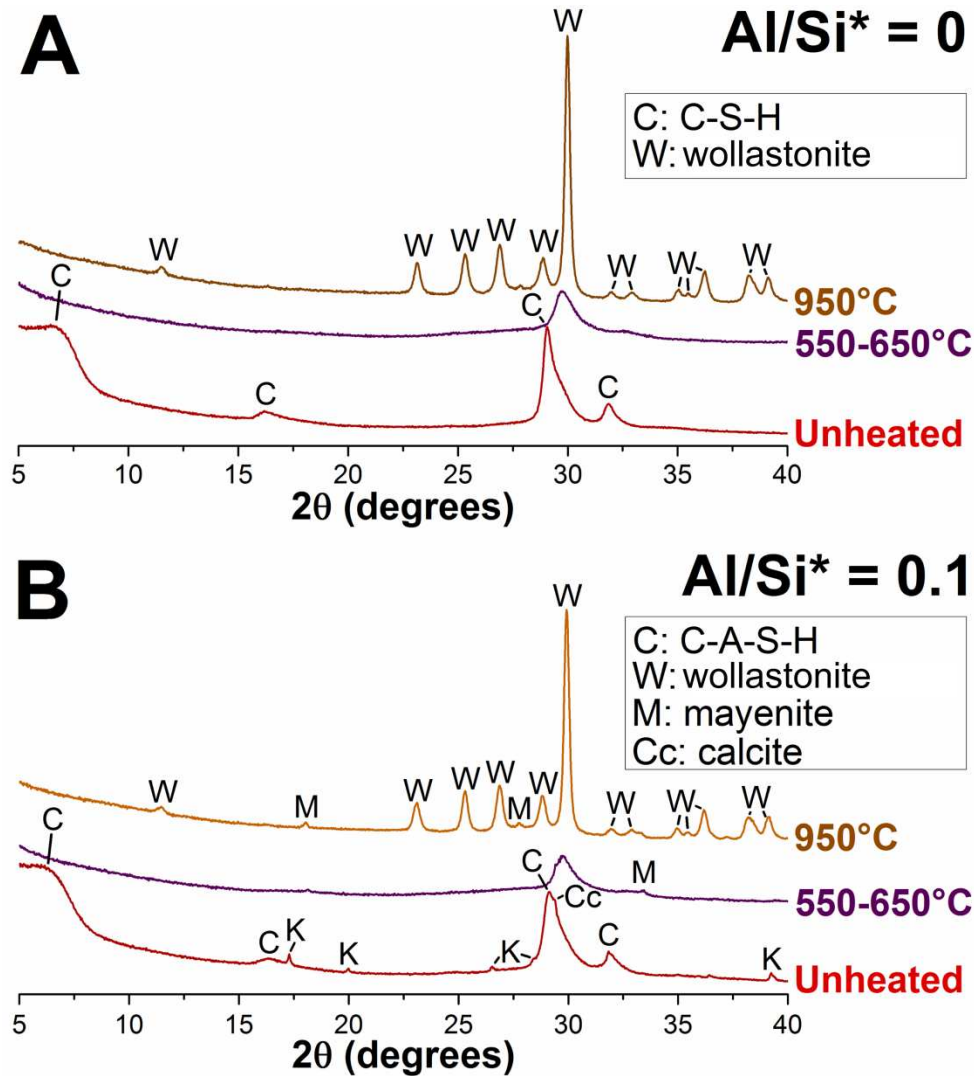


Figure S2. Cu  $K\alpha$  diffractograms of C-(A-)S-H samples equilibrated at 50°C with A) bulk Al/Si = 0 and B) bulk Al/Si = 0.05, heated to the elevated temperatures shown in the plots.

These results confirm the assignment of the differential mass loss peaks at ~380°C and ~500°C (Figure 3) to thermal decomposition of C-(A-)S-H, and assignment of the differential mass loss

peaks at  $\sim 810^\circ\text{C}$  (Figure 3) to the decomposition of C-(A-)S-H to wollastonite. These data also show that the thermal behaviour of the C-(A-)S-H products synthesised here is relatively similar to that of  $14\text{\AA}$  tobermorite [5], which highlights the high level of structural and chemical similarity between these solid phases.

## Appendix S3. Tabulated data relevant to the thermodynamic modelling calculations, including aqueous phase compositions

Aqueous phase compositions and pH results for the C-S-H and C-A-S-H systems are shown in Table S2, and  $\log_{10}(K_{so})$  values for the C-(A-)S-H products calculated here (using the chemical compositions determined by mass balance and reported in Table 3) are shown in Table S3.

Table S2. Aqueous phase compositions and pH results for the C-S-H and C-A-S-H systems.  
Al/Si\* = bulk Al/Si.

Al/Si* = 0					
Temperature (°C)	[Si] (mM)	[Ca] (mM)	[Al] (mM)	[OH <sup>-</sup> ] (mM)	pH †
7	0.025	2.0	0	2.6	11.4
20	0.083	3.2	0	3.9	11.7
50	0.091	2.8	0	5.9	11.7
80	0.11	1.7	0	4.4	11.6
Al/Si* = 0.05					
Temperature (°C)	[Si] (mM)	[Ca] (mM)	[Al] (mM)	[OH <sup>-</sup> ] (mM)	pH †
7	0.046	2.0	0.020	2.9	11.5
20	0.15	2.1	0.020	5.2	11.8
50	0.10	2.4	0.003	5.3	11.6
80	0.073	1.9	b.d.l. ‡	4.2	11.6
Al/Si* = 0.1					
Temperature (°C)	[Si] (mM)	[Ca] (mM)	[Al] (mM)	[OH <sup>-</sup> ] (mM)	pH †
7	0.053	1.7	0.036	2.5	11.4
20	0.11	2.9	0.031	4.2	11.7
50	0.17	1.5	0.028	3.5	11.5
80	0.074	1.7	0.005	4.2	11.6
Al/Si* = 0.15					
Temperature (°C)	[Si] (mM)	[Ca] (mM)	[Al] (mM)	[OH <sup>-</sup> ] (mM)	pH †
7	0.069	1.3	0.043	1.9	11.3
20	0.34	1.3	0.023	3.0	11.5
50	0.32	1.2	0.043	2.1	11.3
80	0.094	1.1	0.039	3.0	11.4

† pH measured at 23°C

‡ b.d.l. = below detection limit for Al (~0.003 mM)

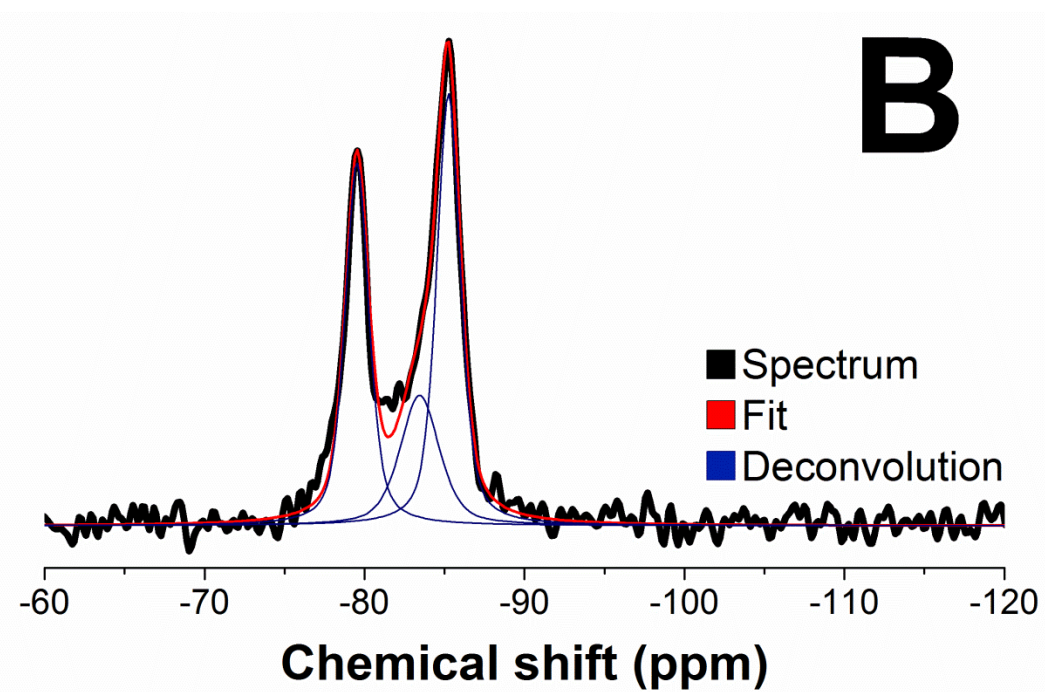
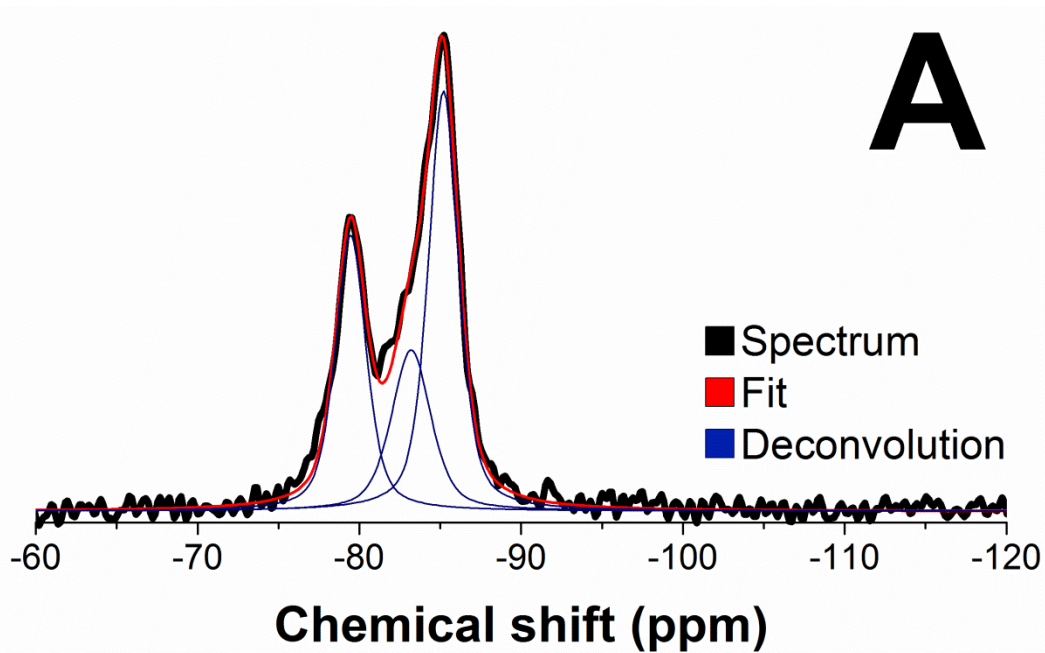
Table S3. Solubility products for the C-(A-)S-H products with chemical compositions given in Table 3, which refer to the reaction given by eq.(6) and  $\text{Ca}^{2+}_{(aq)}$ ,  $\text{SiO}_3^{2-}_{(aq)}$ ,  $\text{AlO}_2^{-}_{(aq)}$ ,  $\text{OH}^{-}_{(aq)}$  and  $\text{H}_2\text{O}_{(l)}$ .  $\text{Al/Si}^* = \text{bulk Al/Si}$ .

<b>Al/Si* = 0</b>	
<b>Temperature (°C)</b>	<b>log<sub>10</sub>(K<sub>so</sub>)</b>
7	-9.98
20	-8.91
50	-8.66
80	-8.80
<b>Al/Si* = 0.05</b>	
<b>Temperature (°C)</b>	<b>log<sub>10</sub>(K<sub>so</sub>)</b>
7	-9.65
20	-8.83
50	-8.82
80	-9.08 †
<b>Al/Si* = 0.1</b>	
<b>Temperature (°C)</b>	<b>log<sub>10</sub>(K<sub>so</sub>)</b>
7	-9.69
20	-8.68
50	-8.64
80	-9.21
<b>Al/Si* = 0.15</b>	
<b>Temperature (°C)</b>	<b>log<sub>10</sub>(K<sub>so</sub>)</b>
7	-9.47
20	-8.52
50	-8.73
80	-9.35

† Solubility product calculated with  $[\text{Al}] = 0.001 \text{ mM}$  because the measured Al concentration was below the detection limit.

## **Appendix S4. Detailed $^{29}\text{Si}$ MAS NMR spectral deconvolution results**

The deconvoluted spectra for the C-S-H systems and the C-A-S-H samples with bulk molar ratios of  $\text{Al/Si} = 0.1$  are shown in Figures S3 and S4 respectively. The results are tabulated in Table S4.



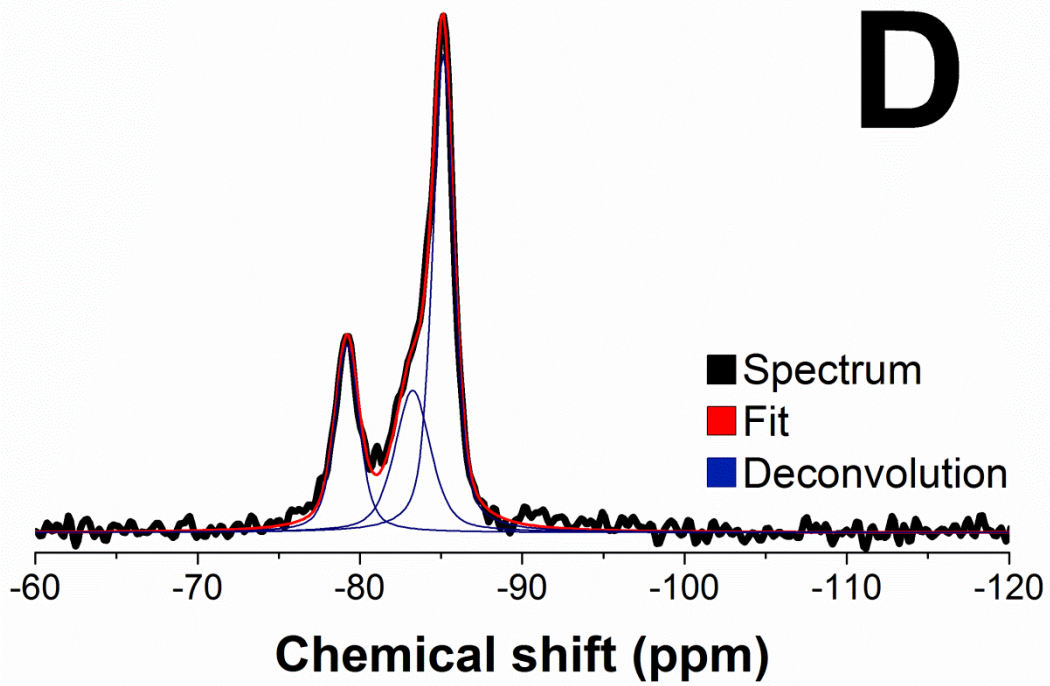
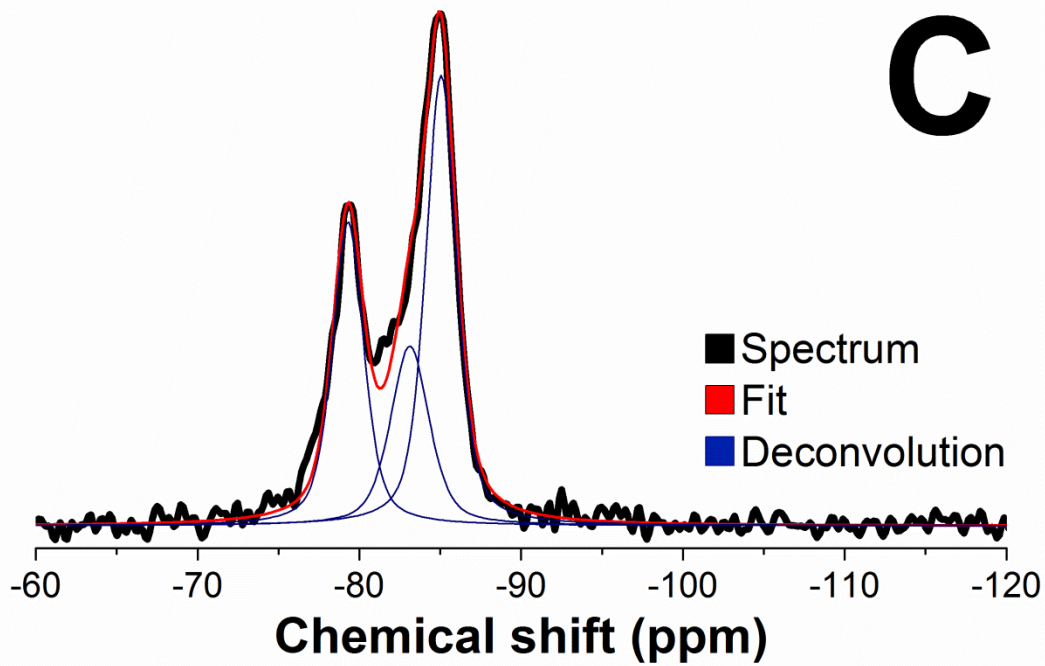
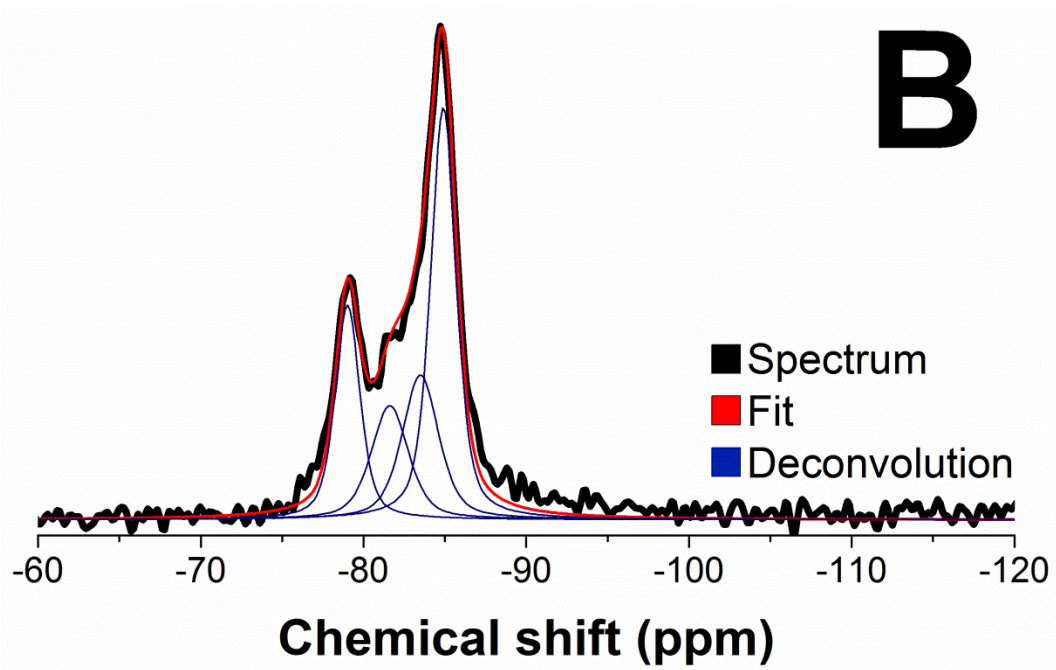
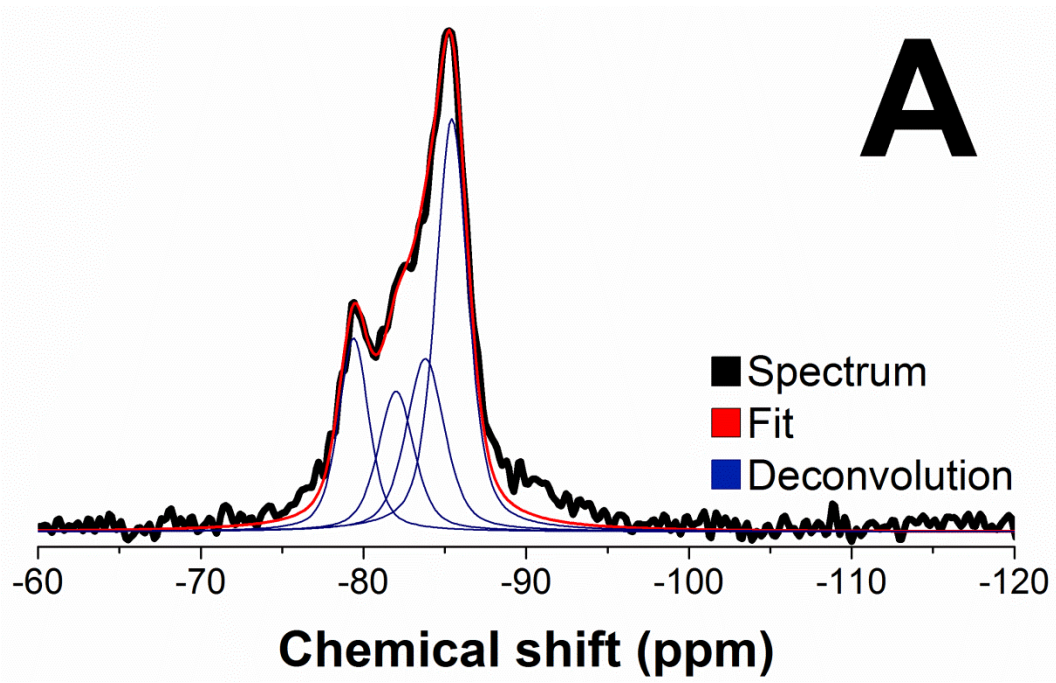


Figure S3. Solid-state  $^{29}\text{Si}$  MAS NMR spectra of the C-S-H systems (bulk Al/Si = 0) equilibrated at A) 7°C, B) 20°C, C) 50°C, D) 80°C.



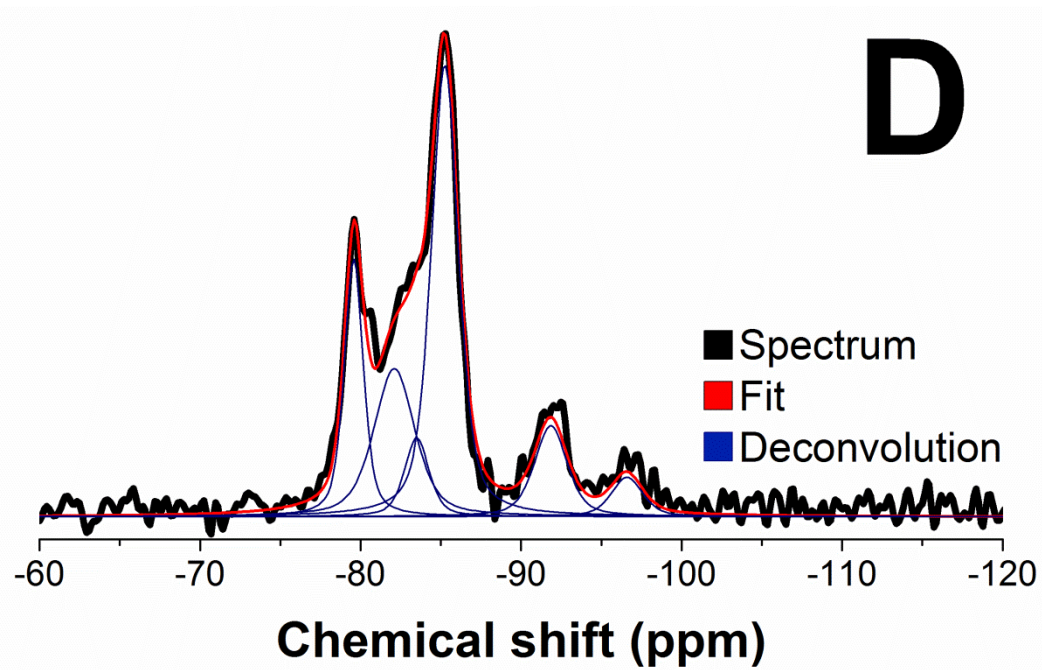
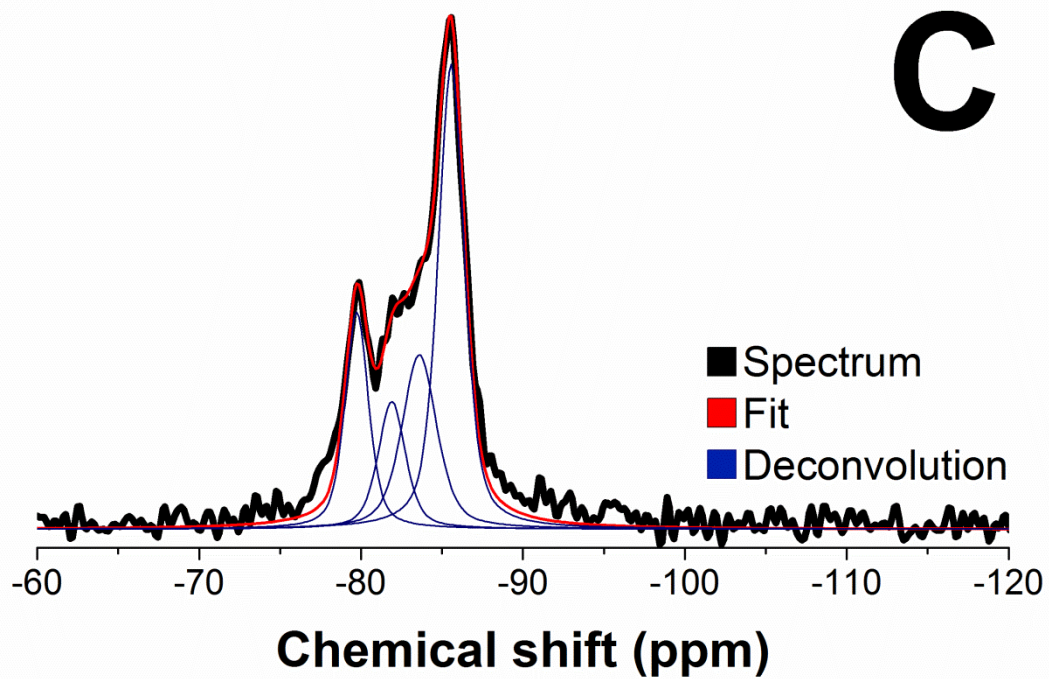


Figure S4. Solid-state  $^{29}\text{Si}$  MAS NMR spectra of the C-A-S-H systems (bulk Al/Si = 0.1) equilibrated at A) 7°C, B) 20°C, C) 50°C, D) 80°C.

Table S4. Deconvolution results for the  $^{29}\text{Si}$  MAS NMR spectra. The estimated error in absolute site percentages is  $\pm 0.03$ . Al/Si\* = bulk Al/Si.

Al/Si*	Temperature (°C)	Q <sup>1</sup>	Q <sup>2</sup> (1Al)	Q <sup>2</sup> <sub>b</sub>	Q <sup>2</sup> <sub>p</sub>	Q <sup>3</sup> (1Al)	Q <sup>3</sup>	Al/Si	MCL
		-79.4 $\pm 0.3$ ppm	-81.9 $\pm 0.2$ ppm	-83.5 $\pm 0.3$ ppm	-85.3 $\pm 0.3$ ppm	-91.9 ppm	-96.6 ppm		
0	7	0.31	0	0.23	0.46	0	0	0	6.5
0	20	0.36	0	0.21	0.43	0	0	0	5.6
0	50	0.32	0	0.23	0.46	0	0	0	6.4
0	80	0.23	0	0.26	0.51	0	0	0	8.8
0.1	7	0.19	0.16	0.22	0.43	0	0	0.081	11.4
0.1	20	0.21	0.17	0.21	0.42	0	0	0.084	10.4
0.1	50	0.20	0.16	0.21	0.43	0	0	0.082	11.0
0.1	80	0.17	0.21	0.07	0.42	0.1	0.04	0.10	19.8

## References in this supporting information file:

1. W. Loewenstein, The distribution of aluminum in the tetrahedra of silicates and aluminates, *Am. Mineral.*, 39 (1954) 92-96.
2. I.G. Richardson, Tobermorite/jennite- and tobermorite/calcium hydroxide-based models for the structure of C-S-H: applicability to hardened pastes of tricalcium silicate,  $\beta$ -dicalcium silicate, Portland cement, and blends of Portland cement with blast-furnace slag, metakaolin, or silica fume, *Cem. Concr. Res.*, 34 (9) (2004) 1733-1777.
3. R.J. Myers, S.A. Bernal, R. San Nicolas, J.L. Provis, Generalized structural description of calcium-sodium aluminosilicate hydrate gels: the cross-linked substituted tobermorite model, *Langmuir*, 29 (2013) 5294-5306.
4. S. Merlino, E. Bonaccorsi, T. Armbruster, The real structures of clinotobermorite and tobermorite 9Å: OD character, polytypes, and structural relationships, *Eur. J. Mineral.*, 12 (2) (2000) 411-429.
5. C. Biagioni, E. Bonaccorsi, S. Merlino, D. Bersani, New data on the thermal behavior of 14 Å tobermorite, *Cem. Concr. Res.*, 49 (2013) 48-54.